

The Role of Pyruvate Dehydrogenase and Acetyl-Coenzyme A Synthetase in Fatty Acid Synthesis in Developing Arabidopsis Seeds¹

Jinshan Ke², Robert H. Behal², Stephanie L. Back, Basil J. Nikolau, Eve Syrkin Wurtele, and David J. Oliver*

Department of Botany (J.K., R.H.B., S.L.B., E.S.W., D.J.O.) and Department of Biochemistry, Biophysics, and Molecular Biology (B.J.N.), Iowa State University, Ames, Iowa 50011

Acetyl-coenzyme A (acetyl-CoA) formed within the plastid is the precursor for the biosynthesis of fatty acids and, through them, a range of important biomolecules. The source of acetyl-CoA in the plastid is not known, but two enzymes are thought to be involved: acetyl-CoA synthetase and plastidic pyruvate dehydrogenase. To determine the importance of these two enzymes in synthesizing acetyl-CoA during lipid accumulation in developing Arabidopsis seeds, we isolated cDNA clones for acetyl-CoA synthetase and for the ptE1 α - and ptE1 β -subunits of plastidic pyruvate dehydrogenase. To our knowledge, this is the first reported acetyl-CoA synthetase sequence from a plant source. The Arabidopsis acetyl-CoA synthetase preprotein has a calculated mass of 76,678 D, an apparent plastid targeting sequence, and the mature protein is a monomer of 70 to 72 kD. During silique development, the spatial and temporal patterns of the ptE1 β mRNA level are very similar to those of the mRNAs for the plastidic heteromeric acetyl-CoA carboxylase subunits. The pattern of ptE1 β mRNA accumulation strongly correlates with the formation of lipid within the developing embryo. In contrast, the level of mRNA for acetyl-CoA synthetase does not correlate in time and space with lipid accumulation. The highest level of accumulation of the mRNA for acetyl-CoA synthetase during silique development is within the funiculus. These mRNA data suggest a predominant role for plastidic pyruvate dehydrogenase in acetyl-CoA formation during lipid synthesis in seeds.

Acetyl-coenzyme A (acetyl-CoA) is a central metabolite in a variety of important physiological processes that link anabolism and catabolism. Acetyl-CoA is a substrate for the TCA cycle and is a precursor for the biosynthesis of fatty acids, waxes, flavonoids, certain amino acids, and isoprenoids formed via HMG-CoA and mevalonate. In addition, acetyl-CoA is the product of the catabolism of fatty acids and some amino acids (e.g. Leu, iso-Leu, and Trp). Despite the importance of these metabolic processes, our understanding of acetyl-CoA generation in plants is rudimentary (Ohlrogge and Browse, 1995). Because acetyl-CoA-requiring metabolism occurs in different subcellular compartments, and because membranes are impermeable to acetyl-CoA, this molecule must either be synthesized within each subcellular compartment where it is required or imported using specific transporters. The question of how acetyl-CoA is generated in plastids is of particular importance in understanding fatty acid biosyn-

thesis, because this process occurs predominantly in this organelle. Considerable evidence indicates the involvement of two enzymes in plastidic acetyl-CoA synthesis, acetyl-CoA synthetase, and plastidic pyruvate dehydrogenase. Two other enzymes, ATP-citrate lyase and acylcarnitine transferase, have also been implicated, but their contribution to acetyl-CoA formation in plastids is not universally accepted.

Over the last 40 years, several mechanisms have been postulated for the physiological source of acetyl-CoA in plastids. Since Smirnov (1960) first made the observation that isolated chloroplasts can synthesize fatty acids from exogenous acetate, acetyl-CoA synthetase (ACS) has been implicated as the source of plastidic acetyl-CoA.

A number of studies with isolated chloroplasts have shown that acetate is the preferred substrate for fatty acid biosynthesis (Roughan et al., 1976, 1979; Roughan, 1978; Schulze-Siebert and Schultz, 1987; Springer and Heise, 1989; Heintze et al., 1990). To explain the possible physiological source of the acetate required by ACS, Stumpf and co-workers (Kuhn et al., 1981; Liedvogel and Stumpf, 1982) suggested that acetate may be generated by a mitochondrial acetyl-CoA hydrolase. They envisioned that this enzyme would hydrolyze mitochondrial acetyl-CoA, and the released acetate could then readily diffuse across membranes and be converted to acetyl-CoA in plastids by ACS. This hypothesis was challenged due

¹ This work was supported by the National Science Foundation (grant no. IBN-9696154), Consortium for Plant Biotechnology, U.S. Department of Agriculture-National Research Initiative (competitive grant no. 97-01912), and the Monsanto Company, and is a publication of the Iowa Agricultural Experiment Station. Microscopy was conducted at the Iowa State University Bessey Microscopy Facility.

² These authors contributed equally to the paper.

* Corresponding author; e-mail doliver@iastate.edu; fax 515-294-1337.

to the difficulties in measuring acetyl-CoA hydrolase activity in mitochondria (Givan and Hodgson, 1983). More recently, however, Zeiher and Randall (1990) have partially purified and characterized this enzyme from pea mitochondria. Alternative sources of acetate have been suggested. These include the combined actions of pyruvate decarboxylase and acetaldehyde dehydrogenase (Cui et al., 1996; op den Camp and Kuhlemeier, 1997; Tadege and Kuhlemeier, 1997) or the action of *O*-acetyl-Ser thiol-lyase in forming Cys from *O*-acetyl-Ser (Leustek and Saito, 1999).

The identification of a plastidic pyruvate dehydrogenase complex (PDC) (Reid et al., 1977; Elias and Givan, 1979; Williams and Randall, 1979; Camp and Randall, 1985; Camp et al., 1988; Randall et al., 1989) led to the concept that plastids may be autonomous in their ability to generate acetyl-CoA from pyruvate (Denyer and Smith, 1988; Randall et al., 1989; Hoppe et al., 1993).

In chloroplasts, pyruvate may be generated from photosynthesis (Denyer and Smith, 1988; Randall et al., 1989; Hoppe et al., 1993), whereas in non-photosynthetic plastids (e.g. leucoplasts of castor bean endosperm) malate and glycolytic metabolism may give rise to pyruvate (Smith et al., 1992). The concept that plastidic acetyl-CoA may be derived from pyruvate has received additional acceptance with the isolation of cDNA clones coding for subunits of plastidic PDC (Johnston et al., 1997).

ATP-citrate lyase, which generates acetyl-CoA in animal cells, has been suggested as the source of acetyl-CoA in plants (Nelson and Rinne, 1975, 1977a, 1977b).

However, studies to ascertain the subcellular location of this enzyme in plants are inconclusive; Fritsch and Beevers (1979) and Ratledge et al. (1997) reported ATP-citrate lyase as plastidic, whereas Kaethner and ap Rees (1985) concluded that ATP-citrate lyase is cytosolic. Therefore, a role for ATP-citrate lyase in generating plastidic acetyl-CoA is unclear.

Last, it has been suggested that acetylcarnitine may be a source of plastidic acetyl-CoA (Masterson et al., 1990a, 1990b; Thomas et al., 1993); however, this mechanism has been challenged (Roughan et al., 1993). Thus, only two enzymes, ACS and plastidic PDC, are known to generate plastidic acetyl-CoA.

The purpose of this study was to determine the contribution of ACS and plastidic PDC to the production of acetyl-CoA in plastids, primarily during seed development in Arabidopsis. To address this question, we isolated Arabidopsis cDNA clones coding for ACS and the ptE1 α - and ptE1 β -subunits of plastidic PDC. We compared the spatial and temporal patterns of ACS and ptE1 β mRNA accumulation with the pattern of lipid accumulation and plastidic acetyl-CoA carboxylase expression (Ke et al., 2000) during seed development. These data indicate that

pyruvate is the main precursor of acetyl-CoA in plastids of developing Arabidopsis seeds.

RESULTS

Cloning of ACS Genic Sequences

ACS has been studied from a variety of organisms and DNA sequences are available for microbial, fungal, and animal ACS genes. These sequences were used to search the Arabidopsis EST database, which resulted in the identification of a single cDNA clone (accession no. N38599) that shared substantial sequence similarity with the known ACS sequences. This cDNA was obtained from the Arabidopsis Biological Research Center (Ohio State University, Columbus) and sequenced. Sequence analysis showed that this clone was only a partial cDNA and a series of 5' cRACE experiments and PCR-based library screens were used to obtain the sequence of the nearly full-length Arabidopsis ACS cDNA (submitted to GenBank as accession no. AF036618).

The protein deduced from this cDNA clone is composed of 693 amino acid residues with a calculated molecular mass of 76,678 D (Fig. 1). The N terminus of the protein has some characteristics of a plastid targeting sequence (von Heinje et al., 1989; von Heinje and Nishikawa, 1991) and computer analysis (PSORT-Sequence Interpretation Tools, GenomeNet, Kyoto, Japan) yielded equivocal results for subcellular targeting. Based on the alignment with the other ACS sequences (Fig. 1), the mature Arabidopsis ACS has an estimated molecular mass of 70 to 72 kD. The value is only approximate because of the lack of sequence identity before the region of high similarity that begins with the Val at residue 54. The sequence identity shared among the Arabidopsis, yeast (44% and 43% identical to yeast ACS1 and ACS2, respectively), and *Escherichia coli* (50% identical) ACS proteins is distributed along the length of the protein (Fig. 1). One of the most conserved regions is between amino acid residues 308 and 319 (Fig. 1); this sequence is the AMP-binding domain. Enzymes that contain this domain form covalent intermediates between their substrate (acetate in the case of ACS) and AMP (Webster, 1965; Toh, 1991).

A portion of the putative Arabidopsis ACS protein was expressed in *E. coli*, and this protein was used to raise a polyclonal antiserum in rabbits. This antiserum was used to support the identification of the ACS cDNA clone. While incubation with preimmune serum had no effect on ACS activity in Arabidopsis leaf extracts, incubation with the antiserum to the putative ACS protein strongly inhibited ACS activity (Fig. 2).

SDS-PAGE and immunoblot analysis of Arabidopsis leaf extracts showed that the ACS antiserum recognizes a single polypeptide with an apparent molecular mass of about 70 kD. This agrees closely with the 70 to 72 kD predicted for the mature form of the protein. Figure 3 shows the results of gel filtration

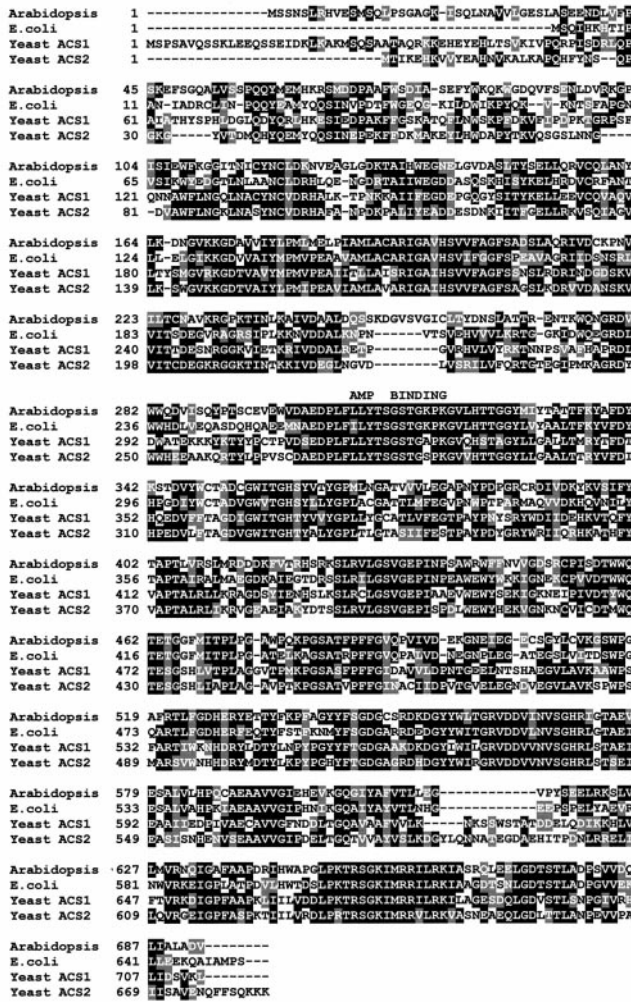


Figure 1. Multiple sequence alignments for ACS proteins from Arabidopsis, yeast, and *E. coli*. The Arabidopsis ACS protein was aligned with the ACS1 and ACS2 proteins from yeast and the ACS protein from *E. coli* using the CLUSTAL W program (Thompson et al., 1994). The alignment was visualized using BOXSHADE (Kay Hoffman and Michael D. Baron; http://ulrec.3.unil.ch/software/BOX_form.html). White letters in a black field represent identical amino acids in two or more sequences. White letters in a gray field indicate conserved substitutions.

analysis of an Arabidopsis extract. The fractions were analyzed for ACS activity and for the presence of the ACS polypeptide. ACS activity and the immunologically identified ACS polypeptide eluted as a single symmetric peak with an apparent molecular mass of approximately 70 kD. These data, together with those from the immunoprecipitation experiment, provide strong correlative support that the ACS enzyme activity is encoded by the putative ACS cDNA clone described in this study. The Arabidopsis ACS protein, therefore, appears to be monomeric.

ACS Activity Is Localized in the Plastids

Protein extracts from purified Arabidopsis chloroplasts showed both ACS enzyme activity and the

70-kD band upon western blotting. To provide a quantitative estimate of the amount of ACS activity localized in the plastid, the activities of ACS and NADP⁺ G3PDH (a chloroplastic marker enzyme [Quail, 1979]) were determined in Arabidopsis protoplasts and in purified chloroplasts isolated from them. In eight experiments, G3PDH activities in the protoplasts and chloroplasts were 0.349 ± 0.023 unit and 0.241 ± 0.023 unit, respectively, whereas ACS activities were 2.699 ± 0.226 units in the protoplast and 1.819 ± 0.108 units in the chloroplasts. A comparison of these data revealed that $97.7\% \pm 5.5\%$ of the ACS activity was localized in the chloroplasts.

Southern-blot analysis of Arabidopsis DNA probed with the ACS cDNA indicated that there is a single ACS gene in Arabidopsis under high-stringency hybridization and wash conditions (Fig. 4). No additional specific bands appeared when the stringency of the hybridization and wash were decreased to 45°C and 0.2× SSC (not shown). The genomic clone for ACS has recently been localized on chromosome 5 (accession no. AB025605).

Cloning and Sequencing of the E1 α - and E1 β -Subunits of Plastidic PDC

Searching the Arabidopsis EST database with the sequences of the ptE1 α and ptE1 β PDC subunits from chloroplasts of the algae *Porphyra purpurea* identified Arabidopsis EST clones for ptE1 α and ptE1 β . Both of the Arabidopsis plastidic E1 β PDC sequences were 68% identical to the plastidic PDC from the red algae and only 37% identical to the mitochondrial PDC from Arabidopsis. The Arabidopsis ptE1 α sequence was 50% and 34% identical to the sequences from *P. purpurea* and the Arabidopsis mitochondrial PDC,

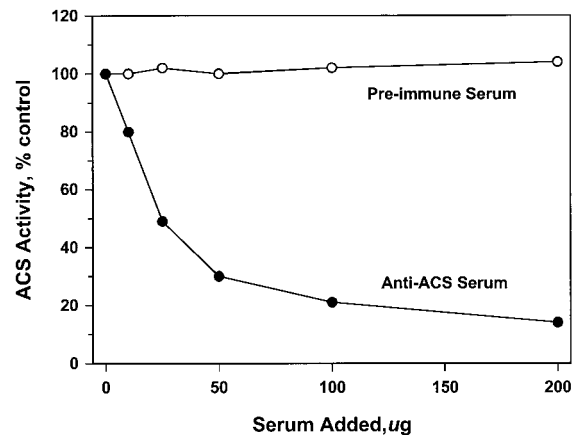


Figure 2. Immunoprecipitation of ACS activity by an antiserum against the transgenic putative ACS protein expressed in *E. coli*. Arabidopsis leaf extract was incubated for 60 min with the indicated concentration of preimmune or antiserum raised against the recombinant protein followed by a 60-min incubation with protein A agarose followed by centrifugation. The remaining ACS activity in the supernatant was then measured.

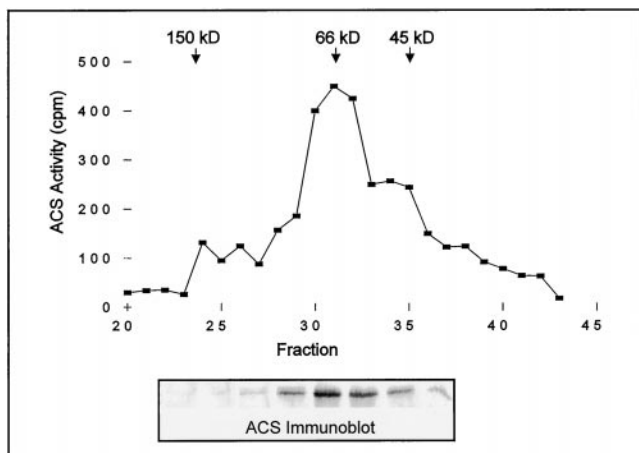


Figure 3. Gel filtration analysis of ACS from Arabidopsis. The 30% to 55% ammonium sulfate precipitate from an Arabidopsis leaf extract was resolved by gel filtration chromatography on a Superdex 220 HR 10–30 column equilibrated in buffer B. The numbers at the top of the figure are molecular mass standards for chromatography. The fractions were analyzed for ACS activity and for the presence of immunoreactive ACS protein. The immunoreactive bands shown at the bottom of the figure contain protein from two column fractions and are aligned with the corresponding fractions.

respectively. Johnston et al. (1997) recently published a detailed characterization of the cDNA clones for the E1 α - and E1 β -subunits of plastidic PDC. Under the stringency used, the mitochondrial clones did not hybridize with the plastid clones.

The cDNAs for the ptE1 α - and ptE1 β -subunits were cloned into pET24-a and simultaneously expressed in *E. coli*. Although the construct was designed to express both PDH subunits simultaneously, only the ptPDH α -subunit accumulated to detectable levels and was present in the insoluble fraction of the *E. coli* lysate. This insoluble fraction was used to produce antibodies in rabbits.

SDS-PAGE and western analysis of Arabidopsis extracts with anti-ptE1 α serum identified a protein of approximately 40 kD. This is the size of the E1 α -subunit of plastidic PDC. No polypeptides of 36 kD (the size of the ptE1 β -subunit) were detected. Mitochondria and chloroplasts were isolated from pea shoots and purified on Percoll gradients. When soluble proteins from these two organelles were analyzed by SDS-PAGE and western blotting, the anti-ptE1 serum recognized the E1 α -subunit of plastidic PDC and mitochondrial PDC with equal sensitivity (data not shown). It was not possible, therefore, to use this antiserum to differentiate between the PDC from the different organelles in whole-cell extracts. When stromal extracts from pea chloroplasts were resolved by gel filtration chromatography and analyzed by western blotting, the ptE1 α fractionated with an apparent molecular mass of 150 kD, possibly representing an $\alpha_2\beta_2$ heterotetramer (data not shown).

ACS and ptE1 β mRNA Accumulation during Silique Formation

RNA was isolated from leaves, flower buds, and flowers, as well as developing siliques 1 to 15 d after flowering (DAF). The accumulation of the ACS and ptE1 β mRNAs was determined by quantitative northern-blot analysis (Fig. 5). In siliques at 1 DAF, ACS mRNA accumulated to a level comparable to that found in leaves, flower buds, and open flowers (Fig. 5). However, as the siliques developed, the accumulation of the ACS mRNA declined, so that by 4 DAF it was at 40% of the peak level and by 15 DAF it was less than 20% of the peak level.

The accumulation pattern of the ptE1 β mRNA showed a much more dynamic response during silique development (Fig. 5). This mRNA accumulated to levels between 2- and 10-fold higher than the ACS mRNA. At the initial stages of silique development (1 DAF), the ptE1 β mRNA accumulated to levels similar to those found in flowers. Subsequently, as the silique expanded, the amount of ptE1 β mRNA reproducibly decreased to about 70% of the initial level by 3 DAF. This was followed by a 3-d period when the ptE1 β mRNA levels increased by about 2-fold, reaching a peak between 6 and 7 DAF. After this peak, the amount of ptE1 β mRNA decreased to reach about 15% to 20% of peak levels by 11 DAF.

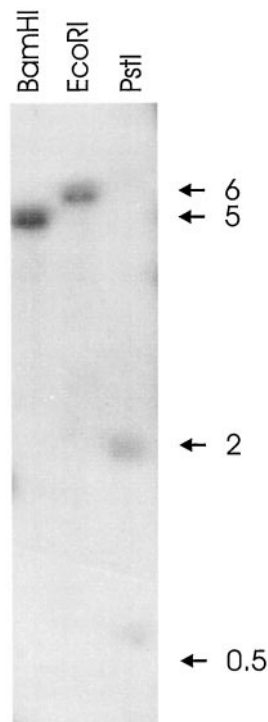


Figure 4. Southern-blot analysis of Arabidopsis DNA probed with the cDNA for ACS. Approximate molecular masses (in kb) are indicated.

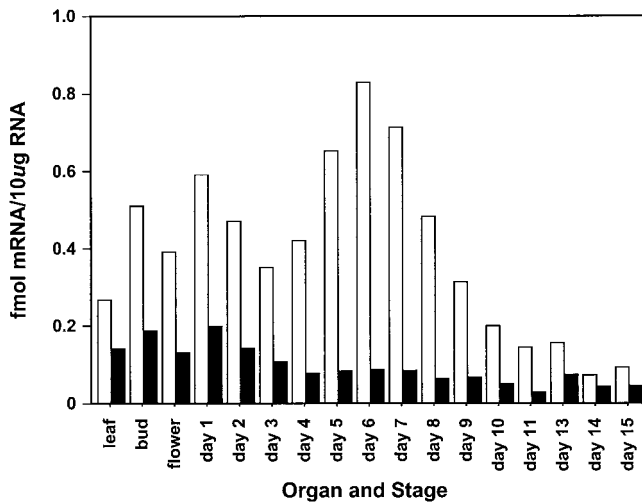


Figure 5. Accumulation of the mRNAs for ACS and ptE1 β in leaves, buds, flowers, and developing siliques (at the indicated DAF) determined by quantitative northern-blot analysis. The data presented are typical of the results from four independent experiments. White bars, Pyruvate dehydrogenase; black bars, ACS.

In Situ Hybridization

To obtain a more comprehensive understanding of the patterns of ACS and pPDH expression during silique development, we examined the cellular distribution of ACS and ptE1 β mRNA accumulation by in situ hybridization. This is significant because each of the different cell types within a silique are likely to have different metabolic demands for plastidic acetyl-CoA. For example, whereas fatty acid biosynthesis is likely to be most active in all growing tissues to satisfy demands for the deposition of membrane lipids required for growth, the developing embryo also synthesizes fatty acids that are deposited in specialized organelles (oleosomes) as triacylglycerol.

Siliques of different ages (1–15 DAF) were collected, sectioned, and probed as described in “Materials and Methods” with radioactively labeled sense and antisense ACS and ptE1 β RNAs (Fig. 6). Figure 6 also shows, for comparison, hybridizations carried out with the carboxyl-transferase- α -subunit of plastidic ACCase (Choi et al., 1995). The plastidic ACCase is composed of four separate subunits, and their spatial accumulation patterns during silique development are indistinguishable from each other (Ke et al., 2000).

At 1 DAF, the ACS mRNA was present throughout the developing silique, but was enriched in the funiculus and ovule (Fig. 6A). By 2 to 3 DAF, the ACS mRNA accumulated predominantly in the funiculus and ovule (Fig. 6, D and T) and its accumulation in the silique wall had declined. In 3-DAF siliques, maximum ACS mRNA accumulation occurred in the globular embryo (Fig. 6D). The accumulation of the ACS mRNA decreased in older siliques (except within the funiculus), so that it was barely detectable

in 5-DAF siliques and undetectable in 7-DAF or older siliques (Fig. 6, G, J, M, and P). The accumulation of the ACS mRNA in the funiculus persisted in siliques up to 12 DAF (data not shown). When seeds were imbibed, there was a large induction in the accumulation of the ACS mRNA in the tip of the radicle of seeds by 1 d after imbibition, and this accumulation continued in the root tip for at least the first 4 d after imbibition (Fig. 6, U–X).

The spatial accumulation pattern of the ptE1 β mRNA was nearly identical to that of the plastidic ACCase subunit mRNAs (Fig. 6; Ke et al., 2000) and was distinct from that of the ACS mRNA. At 1 to 2 DAF, the mRNAs coding for the ptE1 β -subunit and the carboxyl-transferase- α -subunit of plastidic ACCase were evenly distributed throughout the developing silique (Fig. 6, B and C). By 3 DAF, both mRNAs were concentrated within the globular embryo (Fig. 6, E and F), although the plastidic ACCase signal was much greater than that for ptE1 β . Subsequently, the accumulation of these two mRNAs increased substantially in the developing embryos of 5-DAF siliques and peaks in embryos of 7-DAF siliques (Fig. 6, H, I, K, and L). Starting from siliques at 7 DAF, the accumulation of the ptE1 β and carboxyl-transferase- α mRNA decreased until the seed matured at about 12 DAF (Fig. 6, K, L, N, O, Q, and R). In 15-DAF siliques, both mRNA species were undetectable (data not shown).

DISCUSSION

Plants have the capacity to synthesize a diverse set of compounds from acetyl-CoA. Many of these acetyl-CoA-requiring biosynthetic pathways are compartmentalized at the subcellular level, occurring in plastids, mitochondria, or in the cytosol (Liedvogel and Bauerle, 1986). Furthermore, in vivo labeling studies indicate that the source of acetyl-CoA for biosynthetic processes may vary between cell types, between different developmental stages of one tissue, and between different species for the same tissue (Denyer and Smith, 1988; Smith et al., 1992; McCaskill and Croteau, 1995; Eastmond and Rawsthorne, 1997). Therefore, plants appear to have multiple mechanisms for generating acetyl-CoA that are both spatially and temporally separated. Such multiplicity in acetyl-CoA-generating mechanisms would enable plants to differentially regulate the supply of this precursor for the biosynthesis of different phytochemicals.

Characterization of Arabidopsis Acetyl-CoA Synthetase

This report contains the first (to our knowledge) identification of the genic sequence of a putative plant ACS. With the ever-increasing availability of cDNA and genomic DNA sequences in publicly accessible databases, searching for a given protein se-

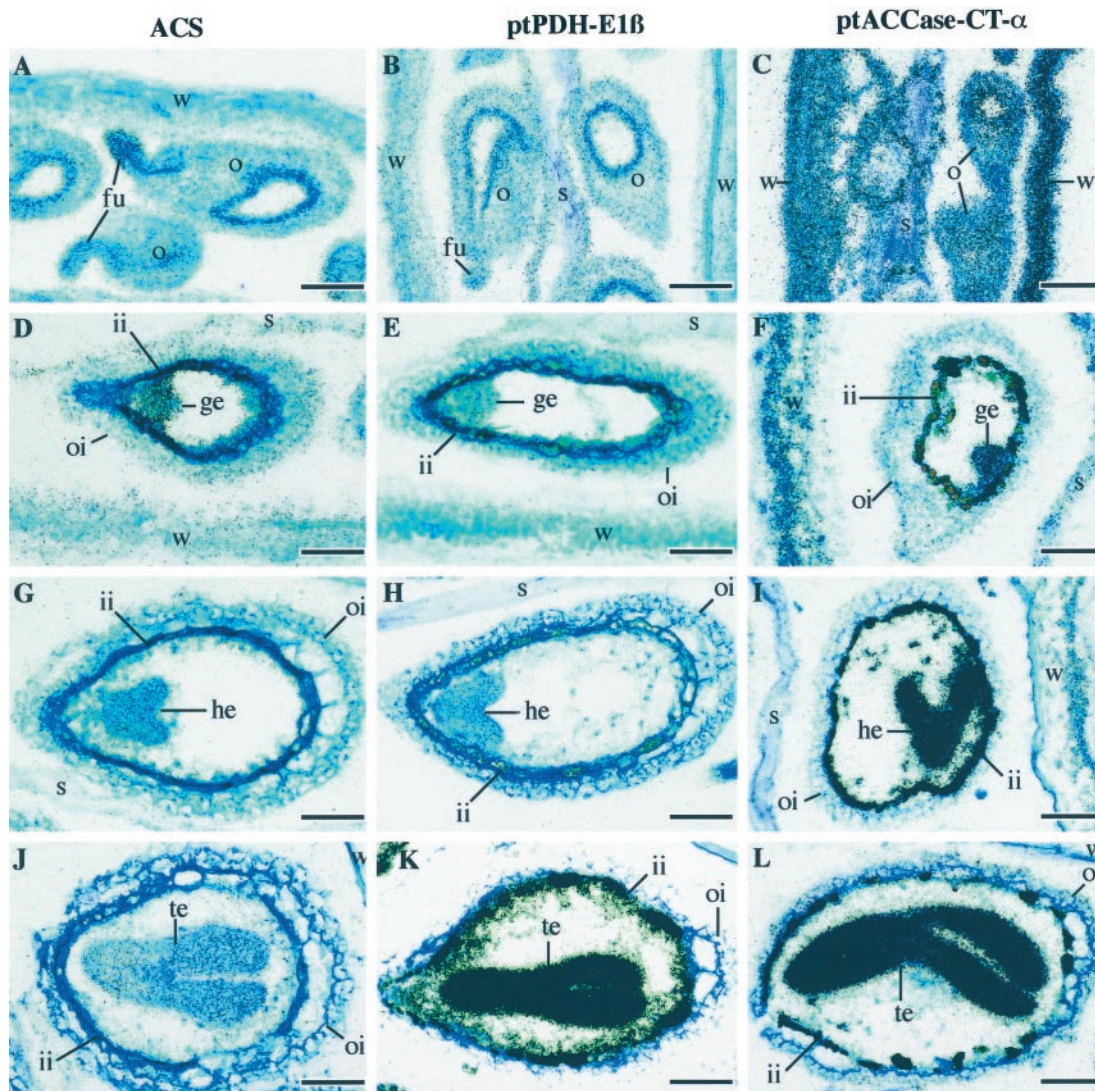


Figure 6. Cellular localization of the mRNA encoding ACS and ptE1 β during development of Arabidopsis siliques and seeds. Tissue sections were hybridized with antisense RNA probes to detect acetyl-CoA synthetase mRNA (12-d exposures) (A, D, G, J, M, P, and T–X) and the ptE1 β mRNA (4-d exposures) (B, E, H, K, N, and Q). The accumulation of the mRNA coding for the carboxyl-transferase- α -subunit of plastidic ACCase (4-d exposures) is shown for comparison (Ke et al., 2000) (C, F, I, L, O, and R). A single, typical control is shown in which sense ptE1 β RNA is used as a probe (S). The control was processed exactly like the experimental sample. A to C, Siliques 1 DAF; D to F and T, siliques 3 DAF; G to I, siliques 5 DAF; J, K, L, (Legend and figure continue on facing page.)

quence by homology-based methods has become common. However, corroborating evidence is necessary to establish whether the deduced amino acid sequence obtained by homology searches is indeed the protein of interest. Strong support of this identification was provided by antiserum raised against the recombinant putative Arabidopsis ACS protein, which specifically inhibited ACS enzymatic activity, co-fractionation of the protein identified by the antiserum and ACS activity by gel filtration chromatography, and co-localization of both the protein and the ACS activity to the plastid.

Computational analyses (GeneRunner, Hastings Software, Hastings on Hudson, NY; and MACAW

[Schuler et al., 1991]) of the ACS cDNA sequence predicted a molecular mass of about 77 kD for the ACS preprotein and about 70 to 72 kD for the mature ACS protein (after removal of the putative plastid-targeting leader). While computer analysis was inconclusive on the presence of a plastid targeting sequence, immunoblot analyses with purified chloroplasts showed that the protein was present in this organelle. The quantitative demonstration that most if not all of the ACS activity resides in the chloroplasts ($97.7\% \pm 5.5\%$) argues strongly for an exclusive plastidic localization of ACS. To date, searches of the Arabidopsis sequence and low-stringency Southern blotting have provided no evidence for a second

cum (Preston et al., 1990) and *Methanothrix soehngenii* (Jetten et al., 1989), are homodimers.

Role of Plastidic PDC in Lipid Synthesis in Developing Seeds

There is limited biochemical evidence as to the relative contribution of ACS and plastidic PDC in acetyl-CoA synthesis in seed plastids. This is in part due to the difficulty associated with the isolation of high-quality plastids from developing embryos and endosperm, together with the difficulty in distinguishing plastidic PDC from mitochondrial PDC activities and plastidic PDC from mitochondrial PDC subunits. Several studies (Miernyk and Dennis, 1983; Liedvogel and Bauerle, 1986; Smith et al., 1992; Kang and Rawsthorne, 1994, 1996) have isolated plastids from oilseed endosperm, embryos, or cotyledons. In each case, ^{14}C -pyruvate was a superior substrate to ^{14}C -acetate for the formation of fatty acids. These results were clearly different from results obtained with chloroplasts isolated from spinach and barley leaves (Roughan et al., 1976; Murphy and Leech, 1977; Roughan, 1978; Schulze-Siebert and Shultz, 1987; Springer and Heise, 1989; Heintze et al., 1990). These latter studies found that higher rates of lipid biosynthesis could be obtained with exogenously supplied ^{14}C -acetate than ^{14}C -pyruvate. Thus, the biochemical evidence is consistent with plastidic PDC being the major source of acetyl-CoA for lipid synthesis in plastids of embryos.

During silique development, the temporal and spatial accumulation patterns of the *ptE1 β* mRNA are consistent with a role for plastidic PDC in fatty acid biosynthesis. While this conclusion is based on mRNA levels, and it is possible that translational and/or post-translational controls would obscure a connection between mRNA levels and in vivo enzyme activities, the conclusion is supported by comparing the accumulation pattern of *ptE1 β* mRNA with that of the mRNAs coding for subunits of one of the key enzymes of fatty acid biosynthesis, plastidic ACCase (Ke et al., 2000). Specifically, during the initial stages of the development of the silique (1 DAF), these mRNAs were evenly distributed among all tissues of this organ. Later, as the silique ceased to elongate, and the embryos within developed through the late-heart and torpedo stages (5–7 DAF), accumulation of these mRNAs reached maximum accumulation within the embryos, but declined in the non-embryo tissues. This pattern of mRNA accumulation is correlated with the expected pattern of fatty acid biosynthesis (Bowman, 1994): At the early stages of the development of the silique, when it is expanding, there should be a relatively high demand for fatty acids among all the cells of this organ, which would be used for the deposition of membranes to support its growth. Later, when growth of the non-embryo tissues of the silique ceases, the embryo itself grows,

and within it large quantities of fatty acids are deposited as triacylglycerol molecules.

Role of ACS

In contrast to the accumulation pattern of *ptE1 β* mRNA, ACS mRNA accumulated with a spatial and temporal pattern that is distinct from that of the plastidic ACCase subunit mRNAs and from the expected pattern of fatty acid accumulation. During silique development, the ACS mRNA accumulated to low levels in the embryos of *Arabidopsis* at times when both plastidic ACCase mRNA accumulation and fatty acid accumulation are at a maximum. Given the caveats about predicting in vivo enzyme activities from mRNA levels, these results indicate that acetyl-CoA synthetase may not be important in providing acetyl-CoA for fatty acid synthesis for oils. Interestingly, within the silique, maximal accumulation of ACS mRNA occurred in the funiculus. Furthermore, within the organs examined, maximal accumulation of ACS mRNA occurred in root tips of radicles of embryos in germinating seeds from 1 to 4 d after imbibition. We surmise that ACS may have a more specialized role in generating plastidic acetyl-CoA in those cells that maximally accumulate this mRNA.

MATERIALS AND METHODS

Cloning of ACS and PDC *ptE1 α* and *ptE1 β* cDNAs from *Arabidopsis*

The *Arabidopsis* EST database was searched using sequences for ACS from yeast and *Escherichia coli*. One *Arabidopsis* sequence (accession no. N38599) was identified that was similar to the known ACS sequences. This clone was obtained from the *Arabidopsis* Biological Research Center and sequenced. It appeared to encode about 40% of ACS, corresponding to the C-terminal ends of the known ACS proteins. A series of cRACE (Maruyama et al., 1995) experiments using mRNA isolated from *Arabidopsis* tissue and PCR amplification of an *Arabidopsis* cDNA library (Wang and Oliver, 1996) allowed us to determine the rest of the cDNA sequence. Once the entire ACS cDNA sequence was determined, an intact clone was amplified from the cDNA library using PCR primers matching the sequences of the 3' and 5' UTRs. This sequence was submitted to GenBank (accession no. AF036618).

cDNA clones coding for the *ptE1 α* - and *ptE1 β* -subunits of the plastidic PDC were identified in a similar manner. In these instances the sequences from the *ptE1 α* - and *ptE1 β* -subunits of plastidic PDC found within the chloroplast genome of the red algae *Porphyra purpurea* were used to search the *Arabidopsis* EST database. Potential clones for *ptE1 α* (accession nos. N65567 and N65566) and *ptE1 β* (accession nos. R29966 and R64987) were obtained from the *Arabidopsis* Biological Research Center and sequenced. cDNA clone N65567 was found to encode for all but approximately 15% of the N terminus of the mature plastid

E1 α ; therefore, it was designated ptE1 α and used in this study. cDNA clone R22966 (designated as ptE1 β -1) contained nearly the entire coding region of ptE1 β and was also used in this study. Since this sequencing was finished, Johnston et al. (1997) also identified these sequences as coding for the E1 α - and E1 β -subunits of plastidic PDC and have provided the sequences for the full-length cDNAs (U80185 and U80186). We also identified a second ptE1 β cDNA (ptE1 β -2) encoding a protein that is 98% identical at the amino acid level to the mature ptE1 β -1 protein (Behal and Oliver, 1999). The sequence of this cDNA was submitted to GenBank as accession number AF167983.

DNA Isolation and Southern Blotting

DNA was isolated using the PHYTOPURE plant DNA extraction kit (Nucleon Biosciences, Coatbridge, UK). Genomic DNA was digested with the appropriate restriction endonucleases. DNA fragments were resolved by agarose gel electrophoresis, denatured with 0.5 M NaOH/1.5 M NaCl, and transferred by buffer flow to genomic blotting membrane (Zeta-Probe, Bio-Rad Laboratories, Hercules, CA). The membrane was briefly neutralized in 0.5 M Tris-HCl, 1.5 M NaCl, pH 8.0, and DNA was immobilized by UV irradiation. The membrane was prehybridized in 7% (w/v) SDS, 1% (w/v) casein, 1 mM EDTA, 0.25 M NaPi, pH 7.4 (Church and Gilbert, 1984), for 1 h at 65°C. Gene-specific ³²P-labeled probe(s) were denatured by incubation at 65°C in the presence of 0.1 M NaOH for 10 min, and were added directly to the prehybridization buffer. The probes were allowed to hybridize to their target sequences overnight at 65°C. Non-specific binding was removed by successive 10-min washes in: 2× SSC/0.1% SDS (w/v), 0.2% SSC/0.1% SDS (w/v), 0.1% SSC/0.1% SDS (w/v) (at room temperature), followed by 0.1% SSC/0.1% SDS (w/v) at 65°C. Hybridizing bands were visualized by exposure to BIOMAX MS film (Eastman-Kodak, Rochester, NY).

Immunological Methods

A portion of the ACS cDNA was PCR amplified from the N38599 EST cDNA clone using primers J9NT1 (gatgaattcggaagtgtgtggtgagcccat) and J9CT1 (atcaagcttcatcacatcg-gcaagtgc), which allowed the resulting fragment to be cloned into the *E. coli* expression vector pMALC-2 (New England Biolabs, Beverly, MA). This clone was transformed into *E. coli*, and expression of the recombinant protein was induced with isopropylthio- β -galactoside. The resulting fusion protein was a chimera consisting of the 264 amino acids at the C terminus of ACS fused to the *E. coli* maltose binding protein. This recombinant protein was isolated from 1-L cultures, purified on an amylose column as per the manufacturer's methods, and assayed for purity by SDS-PAGE. The purified recombinant protein was isolated from the gel and used to immunize rabbits for the production of polyclonal antibodies. The avidity of the resulting antiserum and antibody binding conditions were optimized using a full-length ACS transgenic protein produced from the pET24-a *E. coli* expression vector.

The antisera against the ptE1 subunits were prepared in a similar manner. The cDNA clones for both ptE1 α and ptE1 β were cloned separately into pET24-a vectors. The ptE1 β expression cassette containing the T7-promoter, ptE1 β coding region, and the vector transcriptional terminator was then excised from the ptE1 β clone and incorporated into the ptE1 α pET24-a expression vector. This created a plasmid capable of simultaneously expressing both ptE1 α - and ptE1 β -subunits in *E. coli*. The expressed subunit(s) accumulated as insoluble inclusion bodies that were isolated and purified by SDS-PAGE. Since it was not possible to separate the two recombinant subunits by SDS-PAGE, this protein mixture was used to immunize rabbits.

Protein samples from column fractions, isolated organelles, and whole leaves were resolved by SDS-PAGE in 15% (w/v) acrylamide gels using a mini gel apparatus (Idea Scientific, Minneapolis). For western blotting, proteins were electrophoretically transferred to nitrocellulose in 10 mM 3-(cyclohexylamino)propanesulfonic acid (CAPS), 10% (w/v) methanol, pH 10.5, using a blotting apparatus (Genie, Idea Scientific). Immunodetection of specific proteins was performed following standard protocols (Bolag and Edelstein, 1991).

Characterization of ACS

ACS activity was assayed essentially according to the method of Roughan and Ohlrogge (1994) with some changes. Aliquots (1–10 μ L) of protein were diluted into buffer A (25 mM Tris-HCl and 50 mM KCl, pH 8.5) to a final volume of 90 μ L. Ten microliters of 10× assay mix (2.5 mM CoASH, 25 mM potassium [¹⁻¹⁴C]acetate [3.2×10^6 cpm/ μ mol], 25 mM ATP, 50 mM MgCl₂, and 10 mM dithiothreitol [DTT]) was added to each reaction tube. After incubation for 5 min at room temperature, 75 μ L of the reaction mix was spotted onto a 2.5-cm DE-81 filter circle, which was washed three times for 5 min each in 2% (v/v) acetic acid, rinsed in acetone, dried, and subjected to liquid scintillation counting in the presence of 5 mL of scintillation fluid (Ready Safe, Beckman Instruments, Fullerton, CA).

A crude ACS preparation was made from extracts of mature Arabidopsis leaves. Plants were harvested, washed with cold water, and cooled to 4°C. The tissue was suspended in a minimal volume of buffer A supplemented with 10 mM β -mercaptoethanol, 1 mM benzamidine, 0.1 mM phenylmethylsulfonyl fluoride (PMSF), 0.1% (w/v) defatted bovine serum albumin (BSA), 1 mM EDTA, and 1% (w/v) polyvinylpyrrolidone, and homogenized in a cold Waring blender with several 5-s high-speed bursts. Following filtration through two layers of cheesecloth and two layers of Miracloth (Calbiochem-Novabiochem, La Jolla, CA), the extract was clarified by centrifugation at 25,000g at 4°C for 15 min. The supernatant was subjected to ammonium sulfate precipitation, and ACS activity was recovered in the fraction that precipitated between 30% and 55% saturated ammonium sulfate; ACS activity was stable in this 30% to 55% pellet for several months at –20°C.

A sample of the 30% to 55% ammonium sulfate precipitate was resuspended in a minimal volume of buffer B (25

mm Tris-HCl and 150 mM KCl, pH 8.5) and clarified by centrifugation. A 250- μ L aliquot was applied to a Superdex 220 HR 10-30 column (Amersham-Pharmacia Biotech, Piscataway, NJ) equilibrated in buffer B. Fractions were collected and characterized by enzyme assay and western blotting.

The antiserum raised against the bacterially produced recombinant ACS protein was used to immunoprecipitate the Arabidopsis ACS protein. A crude Arabidopsis extract was incubated with increasing concentrations of antiserum for 60 min. After an additional 60-min incubation with protein-A agarose (Pierce Chemical, Rockford, IL), the extract was centrifuged at 12,000g for 5 min, and the supernatant was assayed for ACS activity.

Preparation of Arabidopsis Chloroplasts and Pea Organellar Extracts

Chloroplasts were isolated from purified Arabidopsis protoplasts as described by Kunst (1998). Protoplast and chloroplast extracts were prepared by incubation with 0.1% (v/v) Triton X-100; the resulting solutions were clarified by centrifugation (12,000g for 10 min) and assayed for ACS and NADP⁺-dependent glyceraldehyde-3-P dehydrogenase (G3PDH) (Worthington, 1988).

Crude pea mitochondria were prepared according to the method of Behal and Oliver (1997). Mitochondria were purified by Percoll gradient centrifugation according to the method of Douce et al. (1987). Chloroplasts were prepared according to the method of Joy and Mills (1987).

RNA Isolation and Northern Blotting

RNA was extracted from Arabidopsis leaves, buds, flowers, and siliques as described previously (Weaver et al., 1995). Non-radioactive sense ACS and ptE1 β RNA concentration standards were made by in vitro transcription from the respective pBSK cDNA clones (Ke et al., 2000). The RNA concentration of the standards was determined from A_{280} and A_{260} , and by comparison with standards of known concentration following ethidium bromide staining of gels. Ten micrograms of RNA isolated from each Arabidopsis sample, along with a range of RNA concentration standards (0.01–10.00 pg), were fractionated by electrophoresis in formaldehyde-containing agarose gels (Ke et al., 2000). After transfer of the RNA to nylon membranes (Magna Lift, MSI, Micron Separations, Westborough, MA), hybridizations were conducted in a buffer containing 50% (v/v) formamide at 65°C for 12 to 16 h using ³²P-labeled probes. ³²P-labeled antisense RNA probes were transcribed from vectors containing the ACS and ptE1 β cDNA inserts. Hybridized membranes were rinsed twice with 2 \times SSC, 2% (w/v) SDS for 10 min each at room temperature, and then washed twice with 0.1 \times SSC, 0.1% (w/v) SDS for 20 min each at 65°C. The membranes were exposed to a phosphor screen (Molecular Dynamics, Sunnyvale, CA) for 4 to 20 h, and the radioactivity in each band was quantified with a phosphor imager (Storm 840, Molecular Dynamics). An entire set of samples (1- to 15-DAF siliques and plant

organs) from two different sets of embryos and plants was repeated twice with similar results; two partial sets of samples were also duplicated with similar results. ACS and ptE1 β mRNA concentrations in each tissue sample were determined by comparing the intensities of the mRNA bands with those of a range of RNA concentration standards (Ke et al., 2000).

In Situ Hybridization

Arabidopsis siliques were harvested daily between 1 and 15 DAF. Siliques were cut into 3- to 4-mm-long pieces, fixed, and sectioned as previously described (Ke et al., 1997). ³⁵S-labeled antisense and sense RNA probes were transcribed from vectors containing cDNA inserts encoding ACS and ptE1 β . cDNA encoding the carboxyl-transferase α -subunit of plastidic ACCase was also used as a probe (Ke et al., 2000). After hybridization and washing, the tissue sections were coated with Kodak NTB2 emulsion, exposed for 2 to 4 d, and developed. Slides were stained with toluidine blue to detect cellular structure. Photographs were taken with a microscope (Orthophan, Leitz, Wetzlar, Germany) using bright-field optics. In situ hybridizations were repeated three or more times, all with similar results. In situ hybridizations to detect ACS and ptE1 β mRNAs were conducted in parallel. Control slides containing sections of the same siliques were hybridized with ³⁵S-labeled sense RNA probes simultaneously with the antisense RNA hybridizations. Virtually no signal was detected in the control slides hybridized with sense RNA probes. For space considerations, the data presented in Figure 6 are from siliques isolated on selected DAF.

Received October 4, 1999; accepted February 15, 2000.

LITERATURE CITED

- Bao X, Pollard M, Ohlrogge J** (1998) The biosynthesis of erucic acid in developing embryos of *Brassica rapa*. *Plant Physiol* **118**: 183–190
- Behal RH, Oliver DJ** (1997) Biochemical and molecular characterization of fumarase from plants: purification and characterization of the enzyme: cloning, sequencing and expression of the gene. *Arch Biochem Biophys* **348**: 65–74
- Behal RH, Oliver DJ** (1999) A second gene encoding the plastidic pyruvate dehydrogenase- β subunit in *Arabidopsis thaliana* (PGR 99–135). *Plant Physiol* **121**: 312
- Bolag DM, Edelman SJ** (1991) *Protein Methods*. Wiley-Liss, New York
- Bowman J** (1994) *Arabidopsis: An Atlas of Morphology and Development*. Springer-Verlag, New York
- Camp PJ, Miernyk JA, Randall DD** (1988) Some kinetic and regulatory properties of the pea chloroplast pyruvate dehydrogenase complex. *Biochim Biophys Acta* **933**: 269–275
- Camp PJ, Randall DD** (1985) Purification and characterization of the pea chloroplast pyruvate dehydrogenase complex. *Plant Physiol* **77**: 571–577

- Choi J-K, Yu F, Wurtele ES, Nikolau BJ** (1995) Molecular cloning and characterization of the cDNA coding for the biotin-containing subunit of the chloroplastic acetyl-coenzyme A carboxylase. *Plant Physiol* **109**: 619–625
- Church GM, Gilbert W** (1984) Genomic sequencing. *Proc Natl Acad Sci USA* **81**: 1991–1995
- Cui X, Wise RP, Schnable PS** (1996) The *rf2* nuclear restorer gene of male-sterile T-cytoplasm maize. *Science* **272**: 1334–1336
- Denyer K, Smith AM** (1988) The capacity of plastids from developing pea cotyledons to synthesise acetyl-CoA. *Planta* **173**: 172–182
- Douce R, Bourguignon J, Brouquisse R, Neuberger M** (1987) Isolation of plant mitochondria: general principles and criteria of integrity. In L Packer, R Douce, eds, *Methods in Enzymology*. Academic Press, San Diego, pp 403–415
- Eastmond PJ, Rawsthorne S** (1997) Developmental changes in substrate utilization for fatty acid synthesis by plastids isolated from oilseed rape embryos. In JP Williams, MU Kahn, NW Lem, eds, *Physiology, Biochemistry, and Molecular Biology of Plant Lipids*. Kluwer Academic Publishers, Boston, pp 66–68
- Elias BA, Givan CV** (1979) Localization of pyruvate dehydrogenase complex in *Pisum sativum* chloroplasts. *Plant Sci Lett* **115**: 115–122
- Frenkel EP, Kitchens RL** (1977) Purification and properties of acetyl coenzyme A synthetase from bakers' yeast. *J Biol Chem* **252**: 504–507
- Fritsch H, Beevers H** (1979) ATP citrate lyase from germinating castor bean endosperm. *Plant Physiol* **63**: 687–691
- Givan CV, Hodgson JM** (1983) Formation of coenzyme A from acetyl-coenzyme A in pea leaf mitochondria: a requirement for oxaloacetate and the absence of hydrolysis. *Plant Sci Lett* **32**: 233–242
- Heintze A, Grolach J, Leuschner C, Hoppe P, Hagelstein P, Schulze-Siebert D, Schultz G** (1990) Plastidic isoprenoid synthesis during chloroplast development. *Plant Physiol* **93**: 1121–1127
- Hoppe P, Heintze A, Riedel A, Creuzer C, Schultz G** (1993) The plastidic 3-phosphoglycerate → acetyl-CoA pathway in barley leaves and its involvement in the synthesis of amino acids, plastidic isoprenoids and fatty acids during chloroplast development. *Planta* **190**: 253–262
- Imesch E, Rous S** (1984) Partial purification of rat liver cytoplasmic acetyl-CoA synthetase: characterization of some properties. *Int J Biochem* **16**: 875–881
- Jetten MS, Stams AJ, Zehnder AJ** (1989) Isolation and characterization of acetyl-coenzyme A synthetase from *Methanothrix soehngenii*. *J Bacteriol* **171**: 5430–5435
- Johnston ML, Luethy MH, Miernyk JA, Randall DD** (1997) Sequencing of *Arabidopsis thaliana* plastid pyruvate dehydrogenase beta subunit. *Biochim Biophys Acta Bioenerg* **1321**: 200–206
- Joy KW, Mills WR** (1987) Purification of chloroplasts using silica sols. In L Packer, R Douce, eds, *Methods in Enzymology*. Academic Press, San Diego, pp 179–188
- Kaethner TM, ap Rees T** (1985) Intracellular location of ATP citrate lyase in leaves of *Pisum sativum* L. *Planta* **163**: 290–294
- Kang F, Rawsthorne S** (1994) Starch and fatty acid synthesis in plastids from developing embryos of oilseed rape. *Plant J* **6**: 795–805
- Kang F, Rawsthorne S** (1996) Metabolism of glucose-6-phosphate and utilization of multiple metabolites for fatty acid synthesis by plastids from developing oilseed rape embryos. *Plants* **199**: 321–327
- Ke J, Choi J-K, Smith M, Horner HT, Nikolau BJ, Wurtele ES** (1997) Structure of the *CAC1* gene and in situ characterization of its expression: the *Arabidopsis thaliana* gene coding for the biotin-containing subunit of the plastidic acetyl-coenzyme A carboxylase. *Plant Physiol* **113**: 357–365
- Ke J, Wen T-N, Nikolau BJ, Wurtele ES** (2000) Coordinate regulation of the nuclear and plastidic genes coding for the subunits of the heteromeric acetyl-CoA carboxylase. *Plant Physiol* **122**: 1057–1071
- Kuhn DN, Knauf M, Stumpf PK** (1981) Subcellular localization of acetyl-CoA synthetase in leaf protoplasts of *Spinacia oleracea* leaf cells. *Arch Biochem Biophys* **209**: 441–450
- Kunst L** (1998) Preparation of physiologically active chloroplasts from Arabidopsis. In J Martinez-Zapater, J Salinas, eds, *Methods in Molecular Biology*. Humana Press, Totowa, NJ, pp 43–48
- Leustek T, Saito K** (1999) Sulfate transport and assimilation in plants. *Plant Physiol* **120**: 637–644
- Liedvogel B, Bauerle R** (1986) Fatty-acid synthesis in chloroplasts from mustard cotyledons: formation of acetyl coenzyme A by intraplastid glycolytic enzymes and a pyruvate dehydrogenase complex. *Planta* **169**: 481–489
- Liedvogel B, Stumpf PK** (1982) Origin of acetate in spinach leaf cells. *Plant Physiol* **69**: 897–903
- Londesborough JC, Yuan SL, Webster LT** (1973) The molecular weight and thiol residues of acetyl coenzyme A synthetase from ox heart mitochondria. *Biochem J* **113**: 23–36
- Maruyama IN, Rakow TL, Maruyama HI** (1995) cRACE: a simple method for identification of the 5' end of mRNAs. *Nucleic Acids Res* **23**: 3796–3797
- Masterson C, Wood C, Thomas DR** (1990a) Inhibition studies on acetyl group incorporation into chloroplast fatty acids. *Plant Cell Environ* **13**: 767–771
- Masterson C, Wood C, Thomas DR** (1990b) L-Acetylcarnitine, a substrate for chloroplast fatty acid synthesis. *Plant Cell Environ* **13**: 755–765
- McCaskill D, Croteau R** (1995) Monoterpene and sesquiterpene biosynthesis in glandular trichomes of peppermint rely exclusively on plastid-derived isopentenyl diphosphate. *Planta* **197**: 49–56
- Miernyk JA, Dennis DT** (1983) The incorporation of glycolytic intermediates into lipids by plastids isolated from the developing endosperm of castor oil seeds. *J Exp Bot* **34**: 712–718
- Murphy DJ, Leech RM** (1977) Lipid biosynthesis from [¹⁴C] bicarbonate, [2-¹⁴C] pyruvate and [1-¹⁴C] acetate

- during photosynthesis by isolated spinach chloroplasts. *FEBS Lett* **77**: 164–168
- Nelson DR, Rinne RW** (1975). Citrate cleavage enzyme from developing soybean cotyledons. *Plant Physiol* **55**: 69–72
- Nelson DR, Rinne RW** (1977a). The role of citrate in lipid synthesis in developing soybean cotyledons. *Plant Cell Physiol* **18**: 1021–1027
- Nelson DR, Rinne RW** (1977b). In vivo citrate studies with developing soybean cotyledons. *Plant Cell Physiol* **18**: 399–404
- Ohlrogge J, Browse J** (1995) Lipid biosynthesis. *Plant Cell* **7**: 957–970
- Ohlrogge J, Pollard MR, Stumpf PK** (1978) Studies on biosynthesis of waxes by developing jojoba seed tissue. *Lipids* **13**: 203–210
- op den Camp RG, Kuhlemeier C** (1997) Aldehyde dehydrogenase in tobacco pollen. *Plant Mol Biol* **35**: 355–365
- Preston GG, Wall JD, Emerich DW** (1990) Purification and properties of acetyl-CoA synthetase from *Bradyrhizobium japonicum* bacteroids. *Biochem J* **267**: 179–183
- Quail PH** (1979) Plant cell fractionation. *Annu Rev Plant Physiol* **30**: 425–484
- Randall DD, Miernyk JA, Fang TK, Budde RJ, Schuller KA** (1989) Regulation of the pyruvate dehydrogenase complexes in plants. In TE Roche, MS Patel, eds, *Alpha-Keto Acid Dehydrogenase Complexes: Organization, Regulation and Biomedical Ramifications*. The New York Academy of Science, New York, pp 192–205
- Ratledge C, Bowater MDV, Taylor PN** (1997) Correlation of ATP/citrate lyase activity with lipid accumulation in developing seeds of *Brassica napus* L. *Lipids* **32**: 7–12
- Reid EE, Thompson P, Lyttle CR, Dennis DT** (1977) Pyruvate dehydrogenase complex from higher plant mitochondria and proplastids. *Plant Physiol* **59**: 842–848
- Roughan G, Post-Beittenmiller D, Ohlrogge J, Browse J** (1993) Is acetylcarnitine a substrate for fatty acid synthesis in plants. *Plant Physiol* **101**: 1157–1162
- Roughan PG** (1978) Acetate is the preferred substrate for long-chain fatty acid synthesis in isolated spinach chloroplasts. *Biochem J* **184**: 565–569
- Roughan PG, Holland R, Slack CR** (1979) On the control of long-chain-fatty acid synthesis in isolated intact spinach chloroplasts. *Biochem J* **184**: 193–202
- Roughan PG, Ohlrogge JB** (1994) On the assay of acetyl-CoA synthetase activity in chloroplasts and leaf extracts. *Anal Biochem* **216**: 77–82
- Roughan PG, Slack CR, Holland R** (1976) High rates of [14 C]acetate incorporation into the lipid of isolated spinach chloroplasts. *Biochem J* **158**: 593–601
- Schuler GC, Altschul SF, Lipman DF** (1991) A workbench for multiple alignment construction and analysis. *Proteins Struct Funct Genet* **9**: 180–190
- Schulze-Siebert C, Schultz G** (1987) β -Carotene synthesis in isolated spinach chloroplasts: its tight linkage to photosynthetic carbon metabolism. *Plant Physiol* **84**: 1233–1237
- Smirnov BP** (1960) The biosynthesis of higher acids from acetate in intact chloroplasts of *Spinacea oleracea* leaves. *Biokhimii* **25**: 419–426
- Smith RG, Gauthier DA, Dennis DT, Turpin DH** (1992) Malate- and pyruvate-dependent fatty acid synthesis in leucoplasts from developing castor endosperm. *Plant Physiol* **98**: 1233–1238
- Springer J, Heise KP** (1989) Comparison of acetate- and pyruvate-dependent fatty-acid synthesis by spinach chloroplasts. *Planta* **177**: 417–421
- Tadege M, Kuhlemeier C** (1997) Aerobic fermentation during tobacco pollen development. *Plant Mol Biol* **35**: 343–354
- Thomas DR, Masterson C, Miernyk JA, Jalil MNH, Ariffin A, Burgess NE, McNeil PH, Fox SR, Toroser D, Wood C** (1993) Carnitine and its role in the plant cell. In PR Shewry, K Stobart, eds, *Seed Storage Compounds, Biosynthesis, Interactions, and Manipulation*. Oxford Science Publishing, Oxford, pp 276–303
- Thompson JD, Higgins DG, Gibson TJ** (1994) CLUSTAL W: improving the sensitivity of progressive multiple sequence alignment through sequence weighting, positions-specific gap penalties and weight matrix choice. *Nucleic Acids Res* **22**: 4673–4680
- Toh H** (1991) Sequence analysis of firefly luciferase family reveals a conservative sequence motif. *Protein Seq Data Anal* **4**: 111–117
- von Heinje G, Nishikawa K** (1991) Chloroplast transit peptides. *FEBS Lett* **278**: 1–3
- von Heinje G, Steppuhn J, Herrmann RG** (1989) Domain structure of mitochondrial and chloroplast targeting peptides. *Eur J Biochem* **180**: 535–545
- Wang CL, Oliver DJ** (1996) Cloning of the cDNA for glutathione synthetase from *Arabidopsis thaliana* and its use to complement a *gsh2* mutant in *S. pombe*. *Plant Mol Biol* **31**: 1093–1104
- Weaver LM, Lebrun L, Franklin A, Huang L, Hoffman N, Wurtele ES, Nikolau BJ** (1995) Molecular cloning of the biotinylated subunit of 3-methylcrotonyl-coenzyme A carboxylase of *Arabidopsis thaliana*. *Plant Physiol* **107**: 1013–1014
- Webster LT** (1965) Studies of the acetyl coenzyme A synthetase reaction. *J Biol Chem* **240**: 4164–4169
- Williams M, Randall DD** (1979) Pyruvate dehydrogenase complex from chloroplasts of *Pisum sativum* L. *Plant Physiol* **64**: 1099–1103
- Worthington CC, ed** (1988) *Worthington Enzyme Manual: Enzymes and Related Biochemicals*. Worthington Biochemical Corporation, Freehold, NJ, pp 172–178
- Zeiber CA, Randall DD** (1990) Identification and characterization of mitochondrial acetyl coenzyme A hydroxylase from *Pisum sativum* L. seedlings. *Plant Physiol* **94**: 20–27